Int. J. Heat Mass Transfer. Vol. 35, No. 2, pp. 481–491, 1992
Printed in Great Britain

0017-9310/92 $5.00 + 0.00


# Characteristics of thermal and flow behavior in the vicinity of discontinuities

DA YU TZOU
Department of Mechanical Engineering, University of New Mexico, Albuquerque, NM 87131, U.S.A.

(*Received* 31 *July* 1990 *and in final form* 19 *February* 1991)

**Abstract**—An asymptotic analysis is applied in this work to study the fundamental behavior of thermal and flow fields in the vicinity of a wedge tip. The emphasis is placed on the physical conditions under which the temperature gradient of the flow field becomes singular at the wedge tip. These conditions are found to be sensitive to the thermal conditions imposed on the wedge surfaces. For natural convection problems, it is found that the $r$-dependencies of the field quantities in the near-tip region are determined by the *eigenvalue* problem for the temperature field, while the eigen-states for the flow velocities are determined by a *boundary* value problem. The reverse situation exists for forced convection problems. A detailed discussion is also provided for the extension of the near-tip solutions to more complicated problems in conjunction with the use of finite element methods.

## 1. INTRODUCTION

WHEN GEOMETRICAL curvature of the physical boundary or the boundary conditions imposed on an engineering system have abrupt changes, singularities may be developed in the neighborhood of discontinuities. A typical example is an isotropic Fourier solid containing a macrocrack subjected to an incoming heat flux or remote temperature gradient [1, 2]. Due to the abrupt change of geometrical curvature at the crack tip, the boundary condition presents a mixed type along the crack line and the radial component of the temperature gradient ($T_{,r}$) presents an $r^{-1/2}$-type of singularity at the crack tip as the radial distance $r$ measured from the crack tip approaches zero. The power of singularity of the temperature gradient is consequently defined as one-half (1/2), which is indeed the negative value of the $r$-dependency of the near-tip temperature gradient. When the effect of thermal conductivity further comes into play, however, the power of singularity of the temperature gradient at the crack tip may change capriciously. For a solid medium with *orthotropic* thermal conductivity [1], as an example, it has been found that the temperature gradient $T_{,r}$ at the crack tip behaves singularly *only if* the ratio of $k_R \equiv k_r/k_\theta > 1/4$. The power of singularity of $T_{,r}$ in this domain is found to be $(2\sqrt{k_R}-1)/2\sqrt{k_R}$, which strongly depends on the ratio of the thermal conductivities in the principal directions of the material orthotropy. When the value of $k_r$ is equal to $k_\theta$, the ratio of $k_R$ reduces to one and the power of singularity being half (1/2) for the isotropic solid is retrieved. For strong directional media with $k_r \gg k_\theta$, the ratio of $k_R$ approaches infinity and the power of singularity has a limit value of one. Other effects such as inhomogeneity and temperature dependence of the thermal conductivity were also studied [3] recently which resulted in different singular behavior of the heat flux vector from that of the temperature gradient at the crack tip. Obviously, a detailed understanding on the singular behavior of the thermal field around discontinuities is important for assessing the thermal and mechanical performance of an engineering system. Especially for those with defects such as cracks developed through service years, such a knowledge directly leads to the estimate of energy intensification [4] in the vicinity of cracks and it is an essential component in the post-damage analysis for engineering systems.

Singularities would also be present in problems of natural convection with discontinuities in either geometry or thermal loading. Natural convective loops [5–8] are a typical example where boundaries with different slopes intersect at the corner of a container. A straight boundary subjected to partial heating [9–12], on the other hand, is another example where distributions of surface heat flux present discontinuities. It has been found that the heat transfer characteristics of the system, such as the nonuniform distributions of the local Nusselt number, are significantly altered by the presence of discontinuities in geometry and/or thermal loading. The wedge flow problems (refer to, for example, ref. [13] for detailed references in the related research) present a geometrical singularity at the wedge vertex but studies in the past mainly focused attention on the formation of boundary layers while a detailed study on the singular behavior of the fluid flow has never been made.

While the existing research develops fundamental understanding of the global behavior of natural convection, the present work focuses attention on the local behavior of thermal and flow fields in the vicinity of the singular point where abrupt changes in geometry and thermal loading conditions exist. The

## NOMENCLATURE

$A, B$ coefficients in equation (24)
$C_n$ $n = 0, 1, 2, \ldots$; coefficients in front of eigenfunctions
$C_p$ heat capacity of fluid [W s kg$^{-1}$ °C$^{-1}$]
$D, E$ coefficients in equation (24)
$f$ energy-bearing capacity of fluid [W m$^{-2}$]
$F_i$ $i = 1, 2$; coefficients in equation (24)
$g$ gravitational constant [m s$^{-2}$]
$h$ heat transfer coefficient [W m$^{-2}$ °C$^{-1}$]
$h', h''$ thermal energy carried by flow velocities [W s m$^{-3}$]
$H_i$ $i = 1$–$6$; coefficients, equation (24)
$k$ isotropic thermal conductivity [W m$^{-1}$ °C$^{-1}$]
$k_r, k_\theta$ principal values of thermal conductivities in the $r$- and $\theta$-directions [W m$^{-1}$ °C$^{-1}$]
$k_R$ ratio of principal values of thermal conductivities, $k_r/k_\theta$
$K_x$ $x \equiv T, u, v$; intensity factors for field quantities $x$
$n$ $0, 1, 2, \ldots$, positive integers
$q$ heat flux component normal to the physical boundary [W m$^{-2}$]
$r$ radial distance measured from the wedge tip or crack tip [m]
$r_i$ $i = 1, 2$; functions of $\beta$ defined in equation (24)
$t$ time [s]
$T$ temperature [°C]
$T_i$ $i = 1$–$7$; nodal temperature in the core element [°C]
$u$ flow velocity in the $r$-direction [m s$^{-1}$]
$u_i, v_i$ $i = 1$–$7$; nodal velocities in the core element [m s$^{-1}$]
$U$ angular distribution of flow velocity in the $r$-direction
$v$ flow velocity in the $\theta$-direction [m s$^{-1}$]
$V$ angular distribution of flow velocity in the $\theta$-direction.

Greek symbols

$\alpha$ wedge angle [deg]
$\beta$ function of $\alpha$, $\beta^2 = (\pi+2\alpha)(\pi+6\alpha)/4\alpha^2$
$\Gamma$ time function
$\Delta$ function of $H_i$ defined in equation (24)
$\varepsilon$ thermal expansion coefficient of fluid [°C$^{-1}$]
$\eta_i$ $i = 1, 2$; coefficients defined in equation (24)
$\theta$ polar angle [deg]
$\Theta$ angular distribution of temperature
$\kappa$ thermal diffusivity [m$^2$ s$^{-1}$]
$\lambda_0, \lambda$ lowest eigenvalues, the $r$-dependency
$\lambda_n$ $n$th eigenvalue
$\mu, \zeta$ Lamé coefficients of viscosity [kg m$^{-1}$ s$^{-1}$]
$\nu$ kinematic viscosity [m$^2$ s$^{-1}$]
$\rho$ fluid density [kg m$^{-3}$].

Subscripts and superscripts

$i$ partial differentiation with respect to $i$
0 quantities at the wedge tip.

emphasis is placed on the physical conditions under which the physical quantity may present a singular behavior. In particular, the natural convection flow pattern in the vicinity of a wedge tip subjected to different thermal boundary conditions on the wedge surfaces will be studied. In the vicinity of the wedge tip, where discontinuities are present in both geometry and thermal loading, the asymptotic analysis employed in previous studies [1–4] will be extended to characterize the fundamental behavior of temperature and flow velocities. It will be demonstrated that two unique features result in the neighborhood of the discontinuity. (1) In momentum transfer, the viscosity effect dominates over the inertia effect. In energy transfer, on the other hand, the effect of heat conduction dominates over that of heat convection by flow velocities. (2) The fundamental behavior of the thermal field is governed by an *eigenvalue* problem while that of the flow field is governed by an associated *boundary* value problem. These situations essentially lead to linearizations of the field equations and facilitate an analytical study on the singular behavior of the thermal and flow fields in the near-tip region.

## 2. CONVECTIVE FLOW PATTERN AROUND A WEDGE TIP

The first problem under consideration is the flow pattern induced by free convection in the vicinity of a wedge tip. As shown previously [1–4], the polar coordinates $(r, \theta)$ are more convenient to be used for the study of near-tip behavior. The three-dimensional configuration of the wedge as well as its two-dimensional idealization are shown in Fig. 1. Due to a non-homogeneous temperature rise in the flow field, additional momentum transfer is induced by the buoyancy force and the momentum equation is

$$u_t + uu_r + (v/r)u_\theta - v^2/r = \nu[u_{rr} + (1/r)u_r - u/r^2 + (1/r^2)u_{\theta\theta} - (2/r^2)v_\theta] + g\varepsilon T\sin(\theta)$$
$$v_t + uv_r + (v/r)v_\theta + uv/r = \nu[v_{rr} + (1/r)v_r - v/r^2 + (1/r^2)v_{\theta\theta} + (2/r^2)u_\theta] + g\varepsilon T\cos(\theta) \quad (1)$$

where $u$ and $v$ are the velocity components in the $r$ and $\theta$ directions, $T$ the temperature above the reference level, $\varepsilon$ the thermal expansion coefficient of the fluid, and subscripts denote partial differentiations. In

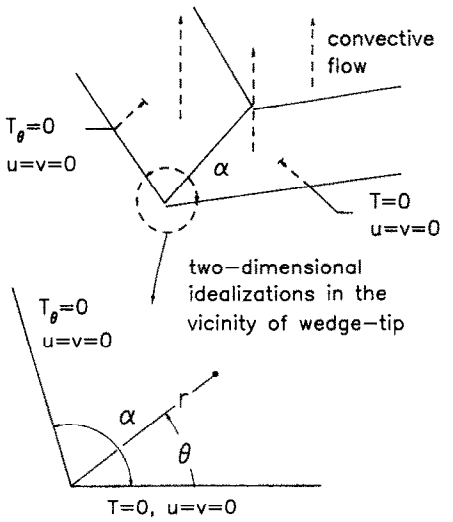


FIG. 1. A wedge subject to different thermal conditions at its surfaces and the polar coordinates centered at the wedge tip.

addition, the velocity components have to satisfy the continuity equation

$$u_r + (1/r)v_\theta = 0 \tag{2}$$

which assumes incompressibility for the fluid flow. The temperature rise $T$ in equation (1) is governed by the conservation of energy in the process of momentum transfer. Mathematically, this is expressed by

$$T_t + uT_r + (v/r)T_\theta = (1/\kappa)[T_{rr} + (1/r)T_r + (1/r^2)T_{\theta\theta}] \tag{3}$$

with $\kappa$ being the thermal diffusivity of the fluid. In these field equations, as usual, we have employed the Boussinesq approximation for the flow density and assumed the absence of energy dissipation [14]. The boundary conditions at the wedge surfaces must be specified in determining the velocity and temperature fields governed by equations (1)–(3). For illustration, we consider

$$T = 0 \quad \text{at} \quad \theta = 0$$
$$T_\theta = 0 \quad \text{at} \quad \theta = \alpha \tag{4}$$

for the thermal field and nonslip conditions

$$u = v = 0 \quad \text{at} \quad \theta = 0 \text{ and } \alpha \tag{5}$$

for the flow field. The wedge angle $\alpha$ is taken to be in the domain from 0 to $\pi$ without loss of generality. The homogeneous type of boundary conditions considered here needs to be discussed. For the thermal and flow fields in the near-tip region, it has been noticed [1–4] that the *magnitude* of the field quantities specified at the boundaries only influences the *intensity* of the physical quantities at the discontinuity while fundamental characteristics such as the spatial distributions in the near-tip region are governed by the corresponding homogeneous conditions. It is in this sense that the near-tip behavior obtained by equations (4) and (5) is applicable to a wedge subject to an incoming heat flux ($T_\theta = q$ at $\theta = \alpha$ for example) or boundary suction or injection ($v = v_0$ at $\theta = \alpha$).

Because the thermal and flow fields in the vicinity of the wedge tip are of major concern, an asymptotic analysis is first made to identify the dominant effects. The continuity equation (2) indicates that the $r$-dependency of the flow velocities $u$ and $v$ must be the same, i.e.

$$\{u(r,\theta,t),\quad v(r,\theta,t)\} = r^{\lambda+1}\{U(\theta), V(\theta)\}\Gamma(t) \tag{6}$$

where a product form for the velocity field has been assumed and the parameter $\lambda$ is temporarily unknown. For the flow field with *bounded* velocity at the wedge tip at $r = 0$, however, a constraint of

$$\lambda + 1 > 0 \tag{7}$$

must be imposed. Substituting equation (6) into equation (1), the $r$-dependency for the terms involved can be categorized as follows:

$$u_t, v_t \sim r^{\lambda+1}$$
$$uu_r, vu_\theta/r, v^2/r, uv_r, vv_\theta/r, uv/r \sim r^{2\lambda+1}$$

and

$$u_{rr}, u_r/r, u/r^2, u_{\theta\theta}/r^2, v_\theta/r^2,$$
$$v_{rr}, v_r/r, v/r^2, v_{\theta\theta}/r^2, u_\theta/r^2 \sim r^{\lambda-1}. \tag{8}$$

Multiplying all the terms in equation (8) by $r^{1-\lambda}$, the terms proportional to $r^{\lambda+1}$, $r^{2\lambda+1}$, and $r^{\lambda-1}$ respectively become $r^2$, $r^{\lambda+2}$, and $r^0$. In the near-tip region with *r approaching zero*, therefore, the time derivative terms $u_t$ and $v_t$ will vanish at a faster rate than the terms proportional to $r^0$ in equation (8) and they can be neglected in the asymptotic expansion of the field equation. Moreover, due to the constraint of equation (7) for the finiteness of the flow velocity at the wedge tip, the value of $\lambda+2$ must be greater than one, which implies that the terms proportional to $r^{2\lambda+1}$ in equation (8) will also vanish at a faster rate in comparison with those proportional to $r^0$ when $r$ approaches zero. From these arguments, it is informative to conclude that the viscous effect in equation (1) dominates over the inertia effect in the near-tip region with $r \to 0$ and the asymptotic expressions for the momentum equation can be written as

$$\nu[u_{rr} + (1/r)u_r - u/r^2 + (1/r^2)u_{\theta\theta} - (2/r^2)v_\theta] + g\varepsilon T\sin(\theta) = 0$$
$$\nu[v_{rr} + (1/r)v_r - v/r^2 + (1/r^2)v_{\theta\theta} + (2/r^2)u_\theta] + g\varepsilon T\cos(\theta) = 0, \quad \text{for } r \to 0. \tag{9}$$

Based on equation (6), the $r$-dependency of the temperature can be determined immediately from equation (9):

$$T(r,\theta,t) \sim r^{\lambda-1}\Theta(\theta)\Gamma(t). \tag{10}$$

Physically, this implies that the buoyancy and viscous

effects in equation (9) are equally important in the process of natural convection. Based on equations (6) and (10) for the flow velocities and temperature, the relative contributions of energy transfer by convection and conduction in equation (3) can be analyzed. Similar to the momentum equation, the $r$-dependency of the terms involved in the energy equation (3) can be summarized as follows:

$$T_t \sim r^{\lambda-1}$$

$$uT_r, vT_\theta/r \sim r^{2\lambda-1}$$

and

$$T_{rr}, T_\theta/r, T_{\theta\theta}/r^2 \sim r^{\lambda-3}. \tag{11}$$

Multiplying all the terms in equation (11) by $r^{3-\lambda}$, similarly, the terms proportional to $r^{\lambda-1}$, $r^{2\lambda-1}$, and $r^{\lambda-3}$ respectively become proportional to $r^2$, $r^{\lambda+2}$, and $r^0$. Due to the constraint of equation (7) for the flow velocity, we may observe that the value of $\lambda+2$ must be greater than one ($\lambda+2>1$) and in the vicinity of the wedge tip with $r$ approaching zero, the terms proportional to $r^{\lambda-3}$ in equation (11) for heat conduction dominate over those for heat convection. The asymptotic form of the energy equation in the near-tip region, therefore, is simply a Laplace equation for heat conduction:

$$T_{rr}+(1/r)T_r+(1/r^2)T_{\theta\theta}=0, \quad \text{for } r\to 0. \tag{12}$$

Through the asymptotic analysis made in the near-tip region, in summary, the momentum and energy equations in the vicinity of the wedge tip are represented by equations (9) and (12). The velocity components $u$ and $v$ and the temperature $T$ in the flow field are to be determined by satisfying the boundary conditions (4) and (5) imposed on the wedge surfaces. By substituting the product forms for the velocities and temperature shown by equations (6) and (10) into equations (4), (5), (9), and (12), due to the equi-dimensionality in the space variable $r$, the governing system can be expressed in terms of the angular distributions $U(\theta)$, $V(\theta)$, and $\Theta(\theta)$:

$$\Theta_{\theta\theta}+(\lambda-1)^2\Theta=0 \tag{13}$$

$$U_{\theta\theta}+[(\lambda+1)^2-1]U-2V_\theta+(g\varepsilon/\nu)\Theta\sin\theta=0$$

$$V_{\theta\theta}+[(\lambda+1)^2-1]V+2U_\theta+(g\varepsilon/\nu)\Theta\cos\theta=0 \tag{14}$$

subject to the boundary conditions

$$\Theta(0)=0, \quad \Theta_\theta(\alpha)=0 \tag{15}$$

for the thermal field and

$$U(0)=U(\alpha)=0, \quad V(0)=V(\alpha)=0 \tag{16}$$

for the flow velocity. They are valid for any function of $\Gamma(t)$ which implies that the near-tip behavior of the thermal and flow fields are essentially *the same* for both transient and steady-state problems. The asymptotic formulation made so far in the near-tip region renders an *eigenvalue* problem to be solved for the eigenvalues $\lambda$. The functions $U(\theta)$, $V(\theta)$, and $\Theta(\theta)$ appear as the eigenfunctions in such a formulation. After the eigenvalue $\lambda$ is successfully found, the $r$-dependency of the velocity and temperature fields can be determined immediately by equations (6) and (10).

In view of equations (13) and (14), we notice that a situation of weak coupling between the thermal and flow fields results. Mathematically, this facilitates determination of the temperature field from equations (13) and (15) in an independent fashion. The results for the eigenvalue $\lambda$ and the eigenfunction $\Theta$ can then be substituted into equations (14) and (16) to determine the eigenfunctions $U(\theta)$ and $V(\theta)$. Equation (13) has the following form of solution:

$$\Theta(\theta)=C_1\cos(\lambda-1)\theta+C_2\sin(\lambda-1)\theta. \tag{17}$$

Employing the boundary conditions (15), the coefficient $C_1$ is zero and the eigen-equation

$$\lambda_n-1=\frac{(2n+1)\pi}{2\alpha} \tag{18}$$

is obtained for $n=0, 1, 2, \ldots$, all the positive integers. The near-tip temperature, from equation (10) and the principle of linear superposition, is thus

$$T(r,\theta)=C_0r^{\lambda_0-1}\sin(\lambda_0-1)\theta+C_1r^{\lambda_1-1}\sin(\lambda_1-1)\theta + C_2r^{\lambda_2-1}\sin(\lambda_2-1)\theta+\cdots \tag{19}$$

with $\lambda_j<\lambda_k$ for $j<k$ according to equation (18). In the near-tip region with $r$ approaching zero, not all the terms in (19) are needed for describing the near-tip behavior of the thermal field. By further inspection in the limit

$$\lim_{r\to 0}[r^{\lambda_j-1}/r^{\lambda_k-1}]=r^{\lambda_j-\lambda_k}\to\infty \quad \text{for } \lambda_j<\lambda_k \tag{20}$$

the terms proportional to $r^{\lambda_k}$ will approach zero at a *faster* rate than those proportional to $r^{\lambda_j}$ as $r\to 0$. In view of equation (19), this implies that the first term indeed dominates over the subsequent terms in the near-tip region with $r$ approaching zero and the asymptotic expression reads as

$$T(r,\theta)\sim C_0r^{\lambda_0-1}\sin(\lambda_0-1)\theta, \quad \text{for } r\to 0 \tag{21}$$

where $\lambda_0=(\pi+2\alpha)/2\alpha$ according to equation (18). Note that the value of $\lambda_0+1=(\pi+4\alpha)/2\alpha$, which is positive definite for any positive value of $\alpha$ and the kinematic constraint of equation (7) for the bounded velocity field is automatically satisfied. Also, equation (21) indicates that only the *lowest* eigenvalue $\lambda_0$ is needed as far as the near-tip behavior of the temperature field is concerned. The corresponding temperature gradient $T_r$ is

$$T_r\sim C_0(\pi/2\alpha)r^{(\pi-2\alpha)/2\alpha}\sin(\pi\theta/2\alpha), \quad \text{for } r\to 0 \tag{22}$$

which presents a *singularity* at $r=0$ for $\alpha>\pi/2$. For the value of $\alpha\in[0,\pi/2]$, both the temperature and its gradient in the $r$-direction are bounded at the wedge tip at $r=0$. For the value of $\alpha\in[\pi/2,\pi]$, the temperature is bounded at the wedge tip while the power of singularity of the temperature gradient $T_r$ is

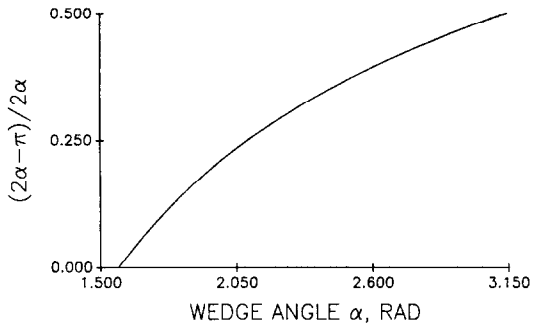


FIG. 2. Power of singularity $(2\alpha-\pi)/2\alpha$ of the temperature gradient varying as a function of the wedge angle, $\pi/2 < \alpha \leqslant \pi$. The case with temperature-gradient-specified condition at $\theta = \alpha$.

$(2\alpha-\pi)/2\alpha$. Figure 2 shows the variation of the power of singularity of $T_r$ vs the wedge angle $\alpha$. When the value of $\alpha$ approaches $\pi$, the power of singularity approaches a limit value of one-half (1/2). For various values of $\alpha$, the corresponding eigenfunctions for the angular variation ($\Theta$) of the near-tip temperature in the respective domains of $\theta \in [0, \alpha]$ are shown in Fig. 3. They are basically the functions of $\sin(\pi\theta/2\alpha)$ shown in equation (22). When the wedge tip temperature gradient switches from a regular to a singular behavior at $\alpha = \pi/2$, no special feature is observed. Note that the asymptotic analysis given here can only provide the fundamental characteristics of the temperature field in the vicinity of the wedge tip. The amplitude $C_0$ of the eigenfunctions in equations (21) and (22), for example, depends on the magnitude of the temperature and heat flux imposed on the wedge surfaces which cannot be determined from the present formulation of eigenvalue problems.

Similar to the thermal field, determination of the flow field in the vicinity of the wedge tip includes the $r$-dependency and angular distributions of the velocity field. According to the result of $\lambda_0 = (\pi+2\alpha)/2\alpha$ obtained from the dominant term in the thermal field, the $r$-dependency of the velocity field in the near-tip region is $\lambda_0+1 = (\pi+4\alpha)/2\alpha$ according to equation (6). Because the value of $\alpha$ is always positive, the velocity vector is bounded at the wedge tip with $r = 0$. Also, because the value of $\lambda_0$ is positive definite, the vorticity vector of the flow field $[0, 0, v_r - u_\theta/r]$ at the wedge tip is bounded as well. The angular distributions $U(\theta)$ and $V(\theta)$ are determined from the eigen-mode of the temperature field. According to equation (21) with the coefficient $C_0$ normalized with $v/g\varepsilon$, the momentum equation (14) in the near-tip region becomes

$$U_{\theta\theta}+\beta^2 U-2V_\theta = -\sin(\pi\theta/2\alpha)\sin(\theta)$$
$$V_{\theta\theta}+\beta^2 V+2U_\theta = -\sin(\pi\theta/2\alpha)\cos(\theta) \quad (23)$$

where the value of $\lambda_0 = (\pi+2\alpha)/2\alpha$ has been used and the parameter $\beta^2 = (\pi+2\alpha)(\pi+6\alpha)/4\alpha^2$. This set of coupled ordinary differential equations has to be solved simultaneously by satisfying the nonslip boundary conditions (16). Rather than an eigenvalue problem, it constitutes a *boundary* value problem to be solved for $U(\theta)$ and $V(\theta)$. The procedure leading to the solutions is lengthy but fundamental [15] and we only present the final results here

$$U(\theta) = C_1\cos(r_1\theta)+C_2\sin(r_1\theta)+C_3\cos(r_2\theta)+C_4\sin(r_2\theta)+D\cos(\eta_1\theta)+E\cos(\eta_2\theta)$$

$$V(\theta) = C_1F_1\sin(r_1\theta)-C_2F_1\cos(r_1\theta)+C_3F_2\sin(r_2\theta)-C_4F_2\cos(r_2\theta)+D\sin(\eta_1\theta)-E\sin(\eta_2\theta),$$

in which

$$C_1 = (H_3H_5-H_2H_6)/\Delta, \quad C_2 = (H_1H_6-H_3H_4)/\Delta,$$
$$\Delta = H_1H_5-H_2H_4, \quad C_3 = -(D+E)-C_1,$$
$$C_4 = -(F_1/F_2)C_2, \quad H_1 = \cos(r_1\alpha)-\cos(r_2\alpha),$$
$$H_2 = \sin(r_1\alpha)-(F_1/F_2)\sin(r_2\alpha),$$
$$H_3 = -D\cos(\eta_1\alpha)-E\cos(\eta_2\alpha)+(D+E)\cos(r_2\alpha),$$
$$H_4 = F_1\sin(r_1\alpha)-F_2\sin(r_2\alpha),$$
$$H_5 = F_1[\cos(r_2\alpha)-\cos(r_1\alpha)],$$
$$H_6 = E\sin(\eta_2\alpha)-D\sin(\eta_1\alpha)+(D+E)F_2\sin(r_2\alpha),$$
$$D = 1/[2(\beta^2-\eta_1^2-2\eta_1)],$$
$$E = -1/[2(\beta^2-\eta_2^2+2\eta_2)],$$
$$\eta_1 = A-1, \quad \eta_2 = A+1, \quad A = \pi/2\alpha,$$
$$F_1 = (\beta^2-r_1^2)/2r_1, \quad F_2 = (\beta^2-r_2^2)/2r_2,$$

and

$$r_1 = [(\beta^2+2)-2(\beta^2+1)^{1/2}]^{1/2},$$
$$r_2 = [(\beta^2+2)+2(\beta^2+1)^{1/2}]^{1/2}. \quad (24)$$

Their graphical representations are shown in Figs. 4–

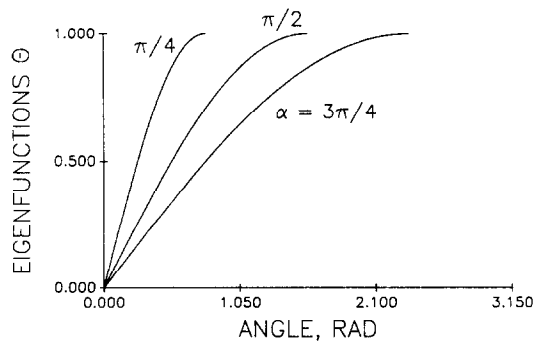


FIG. 3. The eigenfunctions $\Theta$ of temperature in the near-tip region for $\alpha = \pi/4, \pi/2$, and $3\pi/4$. The case with temperature-gradient-specified condition at $\theta = \alpha$.

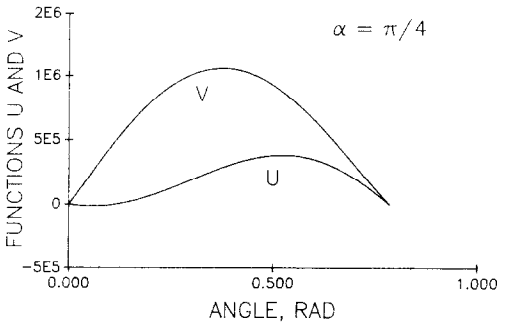


FIG. 4. The angular distributions of flow velocities for $\alpha = \pi/4$. The case with temperature-gradient-specified condition at $\theta = \alpha$.

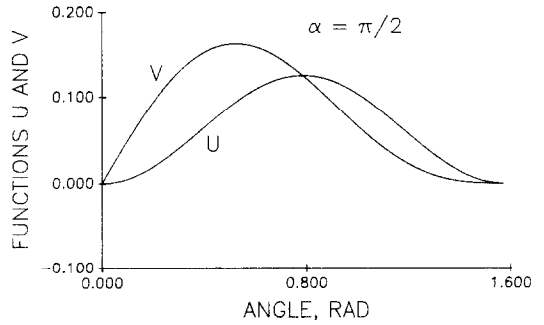


FIG. 5. The angular distributions of flow velocities for $\alpha = \pi/2$. The case with temperature-gradient-specified condition at $\theta = \alpha$.

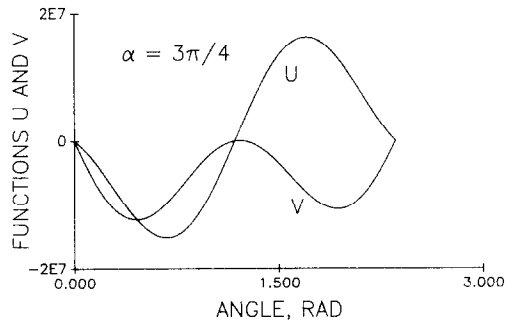


FIG. 6. The angular distributions of flow velocities for $\alpha = 3\pi/4$. The case with temperature-gradient-specified condition at $\theta = \alpha$.

6 for various values of the wedge angle $\alpha$. Note that with the same eigenfunction $\Theta$ for temperature in equation (23), the amplitudes of $U(\theta)$ and $V(\theta)$ for the flow velocities for $\alpha = \pi/4$ and $3\pi/4$ are several orders of magnitude larger than those for $\alpha = \pi/2$. For the case with $\alpha = \pi/4$, the larger amplitude is due to reflection of flow velocities between the wedge surfaces which essentially results in vortex formation. For the case with $\alpha = 3\pi/4$, on the other hand, the larger amplitude is induced by the singularity of the temperature gradient at the wedge tip. A large value of the temperature gradient implies an intensified heat flux supplied thereby into the fluid volume, and the buoyancy effects on the flow velocities are thus more pronounced.

## 3. SINGULARITY OF THE TEMPERATURE GRADIENT

The fundamental characteristics of the temperature gradient in the vicinity of the wedge tip obviously depend on the thermal boundary conditions imposed on the wedge surfaces. In order to develop more understanding of the singular behavior of the temperature gradient in the near-tip region, we further consider an energy-balance condition

$$-kT_\theta/r = f(T,u,v) \quad \text{at} \quad \theta = \alpha \tag{25}$$

at the top wedge surface while the zero-temperature imposed on the bottom surface of the wedge

$$T = 0 \quad \text{at} \quad \theta = 0 \tag{26}$$

remains the same. The function $f$ in equation (25) specifies the energy-bearing capacity of the fluid adjacent to the top wedge surface which is, in general, a complicated function of temperature and flow velocities. In parallel to the asymptotic analysis made so far, it can be first expanded in a Taylor series

$$f(T,u,v) = f_0 + hT + h'u + h''v + O(T^n, u^n, v^n) \tag{27}$$

with $n \geqslant 2$ and $f_0$, $h$, $h'$, $h''$ being constants. By substituting the asymptotic forms for the flow velocities and temperature, equations (6) and (10), into (25) and (27) and taking the limit of $r \to 0$, we observe that the conductive term $kT_\theta/r$ in equation (25) and the 'convective' term $hT$ in equation (27) dominate the near-tip behavior while the other terms involving flow velocities vanish at faster rates. In the near-tip region with $r$ approaching zero, therefore, the asymptotic form of the boundary condition (25) reads as

$$-kT_\theta/r = hT \quad \text{at} \quad \theta = \alpha, \quad \text{for } r \to 0 \tag{28}$$

and the constant $h$ appears to be the overall heat transfer coefficient. The analysis made in the following, therefore, is to study the effect of thermal conductivity $k$ of the wedge medium and the heat transfer coefficient $h$ of the fluid on the singular behavior of the temperature gradient. Because a weak coupling situation exists between the thermal and flow fields, consideration of different thermal boundary conditions on the wedge surfaces does not cause any additional difficulty. With the product form for the near-tip temperature shown by equation (10), the boundary conditions (26) and (28) are expressed in terms of the $\Theta$-function:

$$k\Theta_\theta + h\Theta = 0 \quad \text{at} \quad \theta = \alpha$$
$$\Theta = 0 \quad \text{at} \quad \theta = 0. \tag{29}$$

The solution for $\Theta(\theta)$ is still the same as that shown by equation (17) while the eigen-equation becomes

$$(\lambda - 1)\cos[(\lambda - 1)\alpha] + (h/k)\sin[(\lambda - 1)\alpha] = 0 \tag{30}$$

in this case. Similarly, the coefficient $C_1$ in equation (17) is zero. The *lowest* eigenvalue $\lambda_0$ depicts the near-tip behavior of the thermal field and in the present case, it also depends on the thermal properties ($h$ and $k$) of the system in addition to the geometrical factor $\alpha$. The solution of equation (30) for the lowest eigenvalues $\lambda$ can be found by the Newton–Raphson method [16] and Table 1 shows the results for some typical values of $h/k$ and $\alpha$. Due to the strong effect of thermal properties, we notice that singular behavior of the temperature gradient may not exist at the wedge tip for wedge angles greater than $\pi/2$. For the cases with $\alpha$ being $3\pi/4$ and $h/k$ being 1 and 3, for example, the values of $\lambda-1$ are greater than 1 and the value of $\lambda-2$ is consequently greater than zero. Because the value of $\lambda-2$ (refer to equation (10)) is essentially the $r$-dependency of the temperature gradient $T_r$ in the near-tip region, a positive value of $\lambda-2$ implies a zero value for $T_r$ as the value of $r$ approaches zero. The singularity of temperature gradient at the wedge tip, therefore, is absent in these cases. Analytically, this critical situation can be represented by the condition of

$$\lambda-2=0, \tag{31}$$

or referring to equation (30)

$$h/k=-\cos(\alpha). \tag{32}$$

Figure 7 graphically presents this condition. The value of $\lambda-2$ is positive in the region above the curve and the temperature gradient $T_r$ vanishes as $r\to 0$. Singularity of the temperature gradient exists in the region below the curve and the power of singularity is $2-\lambda$ with $\lambda$ being the lowest eigenvalue satisfying equation (30). The eigenfunction $\Theta(\theta)$ in this case is simply $\sin[(\lambda-1)\theta]$ which is displayed in Fig. 8 for representative values of $h/k$ and $\alpha$. The values of $h/k$ for $\alpha$ being $\pi/4$, $\pi/2$, and $3\pi/4$ are respectively 3, 1, and 0.5 and the corresponding eigenvalues $\lambda$ (refer to Table 1) are 4, 2.39577, and 1.88494. The effects of thermal properties ($h/k$) and geometrical factor ($\alpha$) are

Table 1. The lowest eigenvalues $\lambda$ satisfying the eigenequation (28)

| $\alpha$ values | $h/k$ | The lowest eigenvalue $\lambda$ |
|---|---|---|
| $\pi/4$ | 0.1 | 3.06171 |
| | 0.5 | 3.27541 |
| | 1.0 | 3.48468 |
| | 3.0 | 4.00000 |
| $\pi/2$ | 0.1 | 2.05989 |
| | 0.5 | 2.24340 |
| | 1.0 | 2.39577 |
| | 3.0 | 2.67571 |
| $3\pi/4$ | 0.1 | 1.72485† |
| | 0.5 | 1.88494† |
| | 1.0 | 2.00000 |
| | 3.0 | 2.17491 |

† Cases with $\lambda-2$ negative and the singularity of the temperature gradient ($T_r$) at the wedge tip existing.

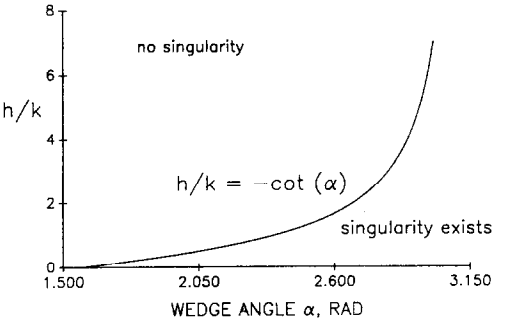


FIG. 7. The envelope for the singular temperature gradient at the wedge tip. Representation in terms of the thermal properties $h/k$ and the geometrical factor $\alpha$.

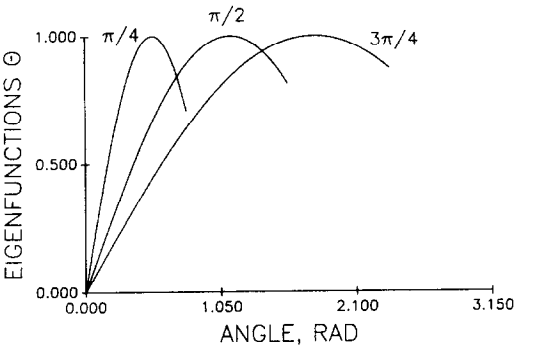


FIG. 8. The eigenfunctions $\Theta$ of temperature in the near-tip region for $\alpha=\pi/4$, $\pi/2$, and $3\pi/4$. The case with energy-balance condition at $\theta=\alpha$.

implicitly implemented in the eigenvalue $\lambda$. When the wedge angle $\alpha$ approaches a value of $\pi$, the wedge becomes a flat plate and the singularity of the temperature gradient, according to equation (32), exists at the wedge tip for the system with finite but nonzero values of $h$ and $k$.

The corresponding flow velocities induced by natural convection in the near-tip region are governed by the following equations:

$$\begin{aligned} U_{\theta\theta}+\beta^2U-2V_\theta &= -\sin[(\lambda-1)\theta]\sin(\theta)\\ V_{\theta\theta}+\beta^2V+2U_\theta &= -\sin[(\lambda-1)\theta]\cos(\theta) \end{aligned} \tag{33}$$

with the eigenfunction $\sin(\pi\theta/2\alpha)$ for temperature in equation (23) replaced by $\sin[(\lambda-1)\theta]$ for the present case. The value of $A$ in equation (24), therefore, is replaced by $(\lambda-1)$ while the rest of the results remain the same. Figures 9–11 display the results of equation (33) for $U(\theta)$ and $V(\theta)$ for various values of $h/k$ and $\alpha$. Basically, they are similar to those shown in Figs. 4–6 but the amplitude of the functions are higher for $\alpha=\pi/4$ and $\pi/2$ and lower for $\alpha=3\pi/4$.

## 4. APPLICATION OF THE NEAR-TIP SOLUTIONS

The asymptotic analysis we have made so far is useful in revealing the fundamental behavior of tem-

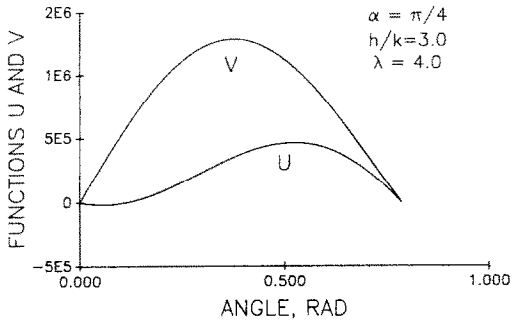


FIG. 9. The angular distributions of flow velocities for $\alpha = \pi/4$. The case with energy-balance condition at $\theta = \alpha$; $h/k = 3.0$ and $\lambda = 4.0$.

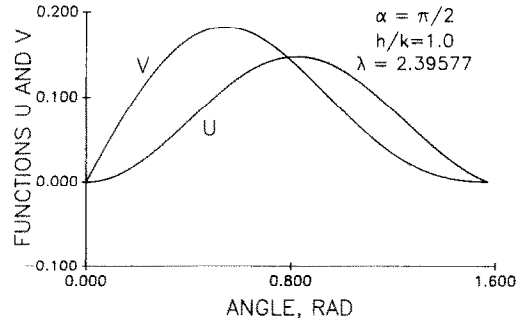


FIG. 10. The angular distributions of flow velocities for $\alpha = \pi/2$. The case with energy-balance condition at $\theta = \alpha$; $h/k = 1.0$ and $\lambda = 2.39577$.

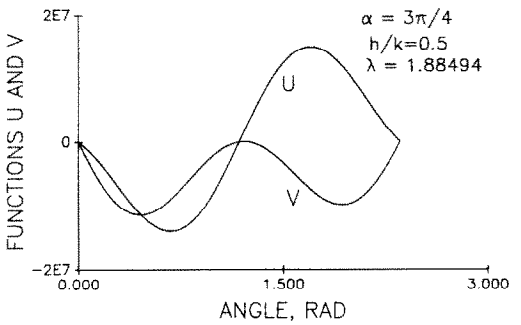


FIG. 11. The angular distributions of flow velocities for $\alpha = 3\pi/4$. The case with energy-balance condition at $\theta = \alpha$; $h/k = 0.5$ and $\lambda = 1.88494$.

perature gradient and flow velocities in the vicinity of the discontinuity. When departing from the discontinuity, however, the inertia effect in momentum transfer and heat convection in energy transfer gradually become important and the nonlinear behavior in the transport processes needs to be considered. In the absence of a singularity, numerical solutions such as finite element or finite difference methods have been demonstrated successfully and widely used in research. In the presence of a singularity, however, a dense mesh pattern containing a lot of discretizing elements or nodes must be used in the neighborhood of the singularity in order to capture the rapid change of the physical quantity. Yet, a quantitative criterion for the necessary number of elements being used in relation to the convergence of numerical solutions is still absent. Moreover, in employing adaptive algorithms based on the change of gradients of physical quantities for generating a finer mesh for convergence, the presence of a singularity may consume all the newly generated elements/nodes and locks up the adaptive process. The temperature gradient shown by equations (22) or (32) is a typical example.

The use of the asymptotic solutions obtained in the vicinity of the singularity could be a practical means to overcome such difficulties. In the neighborhood of the wedge tip, as shown in Fig. 12 where quadrilateral isoparametric finite elements with 12 edge nodes are employed for illustration, the asymptotic solutions for temperature and flow velocities can be implemented on node Nos 1–7:

$$T_i = T_0 + K_T r_0^{\pi/2\alpha} \sin(\pi\theta_i/2\alpha)$$

$$u_i = u_0 + K_u(g\varepsilon/\nu) r_0^{(\pi+4\alpha)/2\alpha} U(\theta_i)$$

$$v_i = v_0 + K_v(g\varepsilon/\nu) r_0^{(\pi+4\alpha)/2\alpha} V(\theta_i) \quad \text{for } i = 1\text{–}7, \tag{34}$$

where the coordinates of $r_0$ and $\theta_i$ for the $i$th node have been substituted into the near-tip solutions obtained in equations (21) and (24). Instead of increasing the number of elements/nodes toward the singularity at the wedge tip for the required convergence and accuracy, the circumference of the circle with radius $r_0$ is the new implicit boundary where the singular behavior of temperature ($T_i$) and/or flow velocities ($u_i$ and $v_i$) obtained analytically are implemented. The numerical effort is then placed on (1) the compatibility of the special core element used in the vicinity of the singularity and the conventional QUAD-12 elements used in the rest of the flow area where nonlinear effects are important and (2) the study on the sensitivity of numerical solutions in relation to the radius $r_0$ selected in equation (34). Along with the nodal temperature and flow velocities at all nodes in the flow discretization, the intensity factors $K_T$, $K_u$, and $K_v$ are obtained as an entirety. From a theoretical point of view, the use of singular core elements could significantly increase the efficiency

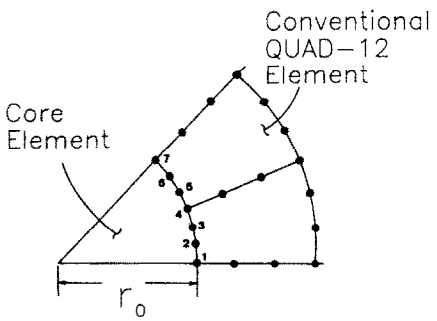


FIG. 12. The concept of core element with implementation of near-tip solutions at node Nos 1–7.

of numerical computations since the singular behavior has been analytically implemented when the discontinuity is closely approached. There is no need to use a lot of elements/nodes to capture the rapid variations of physical quantities thereby. In linear elastic fracture mechanics where a singularity exists at the crack tip in deformation, the advantage of employing the singular core elements in numerical computations has been successfully demonstrated by both the displacement- [17–20] and the stress–displacement hybrid- [21, 22] based formulations. In heat conduction problems, also, the node-shifting technique [4] in calculating the intensity factor of the temperature gradient at the crack tip essentially serves the same purpose by an alternative bi-analytical approach. Implementation of the core element, however, is absolutely nontrivial even with an existing numerical code. The compatibility between the core and the conventional elements and the characteristic value of $r_0$ for the core radius in relation to the accuracy of the numerical solutions strongly depend on the way in which the local elements were assembled and the shape functions used for interpolations. Especially for the present problem with the nonlinear effect of inertia present, how much would the use of core elements improve the numerical accuracy and efficiency is still a research topic worthy of further study.

According to Fourier's law of heat conduction, a singularity in the temperature gradient existing at the wedge tip implies the existence of an intensified heat flux. In the present problem with heat transfer by natural convection, this depicts a situation of energy localization in the flow field which should be avoided for improving the overall performance of heat convection. In optimizing the thermal performance for natural convective loops, for example, the configuration (geometry) with two adjacent walls exposed to temperature and flux-specified conditions (thermal loading) should be avoided, especially those with a blunt vertex angle with $\alpha > \pi/2$. This situation, as demonstrated by equation (32) and shown in Fig. 7, will be dramatically changed when the thermal conditions experienced by the wedge surfaces are different. In the latter case, with the presence of heat convection at the wedge surface, the thermal conductivity of the loop wall and the overall heat transfer coefficient of the fluid (thermal properties) further interact with the geometrical factor of vertex angle $\alpha$ in the evolution of energy localization and optimization of the thermal system becomes quite a complicated subject matter of research. The over-simplified boundary conditions, equations (4) and (29), in this work are only employed for illustrating the existence of a singularity and consequently the energy localization. In modeling real situations in engineering systems, the boundary conditions may be much more complicated than those considered in this analysis and the performance curve of the system should involve all the physical factors in geometry, thermal loading, and thermal properties of the media.

## 5. CONCLUSIONS

An asymptotic analysis has been made to study the thermal and flow behavior in the vicinity of a wedge tip where discontinuities in geometry and physical boundary conditions are present. Generally speaking, the results obtained in this analysis for $\alpha = \pi/2$ could be applied to containers with right corners and those for $\alpha = \pi$ could be applied to containers subject to partial heating on their boundaries. The analysis demonstrates that in the near-tip region with $r$ approaching zero, the inertia effect in the flow field and the convective transfer by flow velocities in the thermal field are higher order effects in comparison with, respectively, the viscous and the conductive effects in the momentum and the energy equations. From a mathematical point of view, this decouples the flow velocity from the energy equation and an *eigenvalue* problem is rendered for determining the thermal field while a *boundary* value problem is rendered for determining the flow field. The *lowest* eigenvalue resulting from the eigenvalue problem depicts the $r$-dependency of both the thermal and flow fields in the near-tip region. For the wedge subject to a temperature-specified condition at the bottom surface ($\theta = 0$) and a flux-specified condition at the top surface ($\theta = \alpha$), the temperature gradient presents a singularity only if the wedge angle $\alpha$ is in the domain from $\pi/2$ to $\pi$. The power of singularity is $(2\alpha - \pi)/2\alpha$. For the same wedge surfaces subject to an energy-balance condition at the top, the singular behavior of the temperature gradient also depends on the thermal properties (the ratio of $h/k$) of the physical system. Equation (32) depicts the conditions under which the temperature gradient at the wedge tip becomes singular and Fig. 7 displays such an envelope in terms of the ratio of $h/k$ vs the wedge angle $\alpha$. In the presence of a singularity of the temperature gradient at the wedge tip, generally speaking, the energy transfer through the top surface of the wedge *reduces* the magnitude of the power of singularity in comparison with the case subject to a gradient-specified condition. For the case of $\alpha = 3\pi/4$ in Table 1, for example, the power of singularity of the temperature gradient at the wedge tip is 1/3 for a flux-specified wedge surface while it is respectively 0.27515 and 0.11506 for the surface subject to an energy balance condition with $h/k = 0.1$ and 0.5. Besides, for natural convection problems considered so far, the velocity and the vorticity vectors of the flow field are found to be bounded at the wedge tip. No singularity would be induced by the non-isothermal expansion of the fluid volume.

To be noted is the fact that the singularity of the temperature gradient at the wedge tip is indeed contributed to by both geometrical and physical discontinuities. For the same wedge subject to temperature-specified conditions on *both* surfaces, $\Theta(\alpha) = \Theta_0$ and $\Theta(0) = 0$ for example, the same procedure will render a result of $\lambda_0$ (the lowest eigenvalue) equal to two for a nontrivial solution of $\Theta(\theta)$. The $r$-depen-

dency $(\lambda-2)$ of the temperature gradient $T_r$ at $r=0$, therefore, is zero and there exists no singularity in the entire domain of the wedge angle $\alpha$ although the abrupt change of geometrical curvature still exists at the wedge tip in this case. It is thus clear that the singular behavior of the temperature gradient at the wedge tip is a combined result of the geometrical configuration, thermal properties, and the way in which the physical system is thermally loaded.

For fluid passing over a flat plate with finite length, similar situations exist in the wake region adjacent to the trailing edge of the plate. By the same concept developed in this work, the momentum and energy equations in this case of force convection turn out to be

$$u_{rr}+(1/r)u_r-u/r^2+(1/r^2)u_{\theta\theta}-(2/r^2)v_\theta=0$$
$$v_{rr}+(1/r)v_r-v/r^2+(1/r^2)v_{\theta\theta}+(2/r^2)u_\theta=0, \qquad (35)$$

and

$$T_{rr}+(1/r)T_r+(1/r^2)T_{\theta\theta}=-(\kappa/\rho C_p)\{\mu\{2[u_r^2+(v_\theta/r+u/r)^2]+[u_\theta/r+v_r-v/r]^2\}+\zeta\{u_r+v_\theta/r+u/r\}^2\}, \quad \text{for } r\to 0 \qquad (36)$$

which are respectively in correspondence with equations (9) and (12) derived previously. There are two special features behind equations (35) and (36). In the momentum equation (35), it indicates that the flow inertia and buoyancy force are lower order effects in comparison with the viscosity effects. In the energy equation (36), on the other hand, it indicates that the magnitude of energy dissipation due to fluid viscosity is equally weighted with respect to that of heat conduction. Bearing this in mind and with the assistance of the product forms for flow velocities shown in equation (6), the $r$-dependency of the temperature in the vicinity of the trailing edge of the plate can be derived as $2(\lambda-1)$, i.e.

$$T(r,\theta)\sim r^{2(\lambda+1)}\Theta(\theta)\Gamma(t), \qquad (37)$$

and the corresponding equations to (13) and (14) are

$$U_{\theta\theta}+[\lambda(\lambda+2)]U=2V_\theta$$
$$V_{\theta\theta}+[\lambda(\lambda+2)]V=-2U_\theta \qquad (38)$$

$$\Theta_{\theta\theta}+[4(\lambda+1)^2]\Theta=-(\kappa/\rho C_p)\{\mu\{2[(\lambda+1)^2U^2+(V_\theta+U)^2]+[U_\theta+\lambda V]^2\}+\zeta\{V_\theta+(\lambda+2)U\}^2\}, \quad \text{for } r\to 0 \qquad (39)$$

in the present case. Equations (38) and (39) appear to be counterparts of equations (13) and (14). The temperature in this case is decoupled from the momentum equation and the flow velocities are determined in an independent fashion rather than the temperature in the previous case. Subjected to the appropriate boundary conditions specified at the plate surface ($U=V=0$ for example) and in the wake region ($U_\theta=0$ and $V=0$ [13]), the $r$-dependency can thus be determined from the *eigenvalue* system governing the flow field and the modal response of temperature is consequently obtained by solving the *boundary* value problem represented by equation (39). Along with more general conditions considered in the wake region such as cavitation, this class of interesting problems will be discussed in the near future.

## REFERENCES


1. D. Y. Tzou, Thermal shock waves induced by a moving crack, *ASME J. Heat Transfer* **112,** 21–27 (1990).
2. D. Y. Tzou, The singular behavior of the temperature gradient in the vicinity of a macrocrack tip, *Int. J. Heat Mass Transfer* **33,** 2625–2630 (1991).
3. D. Y. Tzou, Diminution of temperature gradient at the crack tip due to the effect of thermal conductivity, *ASME J. Heat Transfer* (accepted for publication).
4. D. Y. Tzou, On the use of node-shifting techniques for the intensity factor of temperature gradient at a macrocrack tip, *J. Numer. Heat Transfer* **19(A),** 237–253 (1991).
5. A. Metrol and R. Greif, A review of natural circulation loops. In *Natural Convection: Fundamentals and Applications* (Edited by W. Aung, S. Kakaç and R. Viskanta), pp. 1033–1071. Hemisphere, New York (1985).
6. E. Ramos, A. Castrejon and M. Gordon, Natural convection in a two-dimensional square loop, *Int. J. Heat Mass Transfer* **33,** 917–930 (1990).
7. A. Mertol, R. Greif and Y. Zvirin, Two-dimensional study of heat transfer and fluid flow in a natural convection loop, *ASME J. Heat Transfer* **104,** 508–514 (1982).
8. J. E. Hart, A new analysis of a closed loop thermosyphon, *Int. J. Heat Mass Transfer* **27,** 125–136 (1984).
9. S. H. Park and C. L. Tien, An approximate analysis for convective heat transfer on thermally nonuniform surfaces, *ASME J. Heat Transfer* **112,** 952–958 (1990).
10. M. Kelleher, Free convection from a vertical plate with discontinuous wall temperature, *ASME J. Heat Transfer* **93,** 349–356 (1971).
11. S. Lee and M. M. Yovanovich, Natural convection from a vertical plate with step changes in surface heat flux, *ASME HTD* **107,** 239–247 (1989).
12. J. A. Schetz and R. Eichhorn, Natural convection with discontinuous wall-temperature variations, *J. Fluid Mech.* **18,** 167–176 (1964).
13. D. Meksyn, *New Methods in Laminar Boundary Layer Theory*, Chap. VIII. Pergamon Press, London (1964).
14. C.-S. Yih, *Fluid Mechanics, A Concise Introduction to the Theory*, Chap. 8. McGraw-Hill, New York (1968).
15. F. B. Hildebrand, *Advanced Calculus for Applications*, Chap. 1. Prentice-Hall, Englewood Cliffs, New Jersey (1974).
16. B. Carnahan, H. A. Luther and J. O. Wilkes, *Applied Numerical Methods*, Chap. 3. Wiley, New York (1969).
17. P. D. Hilton and L. N. Gifford, Jr. Finite element fracture mechanics analysis of two-dimensional and axisymmetric elastic and elastic–plastic cracked structures, David Taylor Naval Ship Research and Development Center, DTNSRDC Report 4493 (1974).
18. S. N. Atluri, A. S. Kobayashi and M. Nakagaki, Fracture mechanics application of an assumed displacement finite element procedure, *AIAA J.* **43,** 734–739 (1975).
19. R. S. Barsoum, On the use of isoparametric finite elements in linear fracture mechanics, *Int. J. Numer. Meth. Engng* **10,** 25–37 (1976).
20. D. Y. Tzou and G. C. Sih, Dynamic elastic–plastic analysis (DEPA), Technical Report of the Institute of Frac-

ture and Solid Mechanics, IFSM-86-140, Lehigh University, Bethlehem, Pennsylvania (1986).
21. T. H. H. Pian, P. Tong and C. Luk, Elastic crack analysis by a finite element hybrid method, *Third Air Force Conf. on Matrix Methods in Structural Mechanics*, Ohio (November 1971).
22. J. Ahmad and F. T. C. Loo, A mixed finite element for accurate crack tip stress analysis. In *Fracture Mechanics in Engineering Application* (Edited by G. C. Sih and S. R. Valluri), pp. 693–704. Sijthoff & Noordhoff, The Netherlands (1979).

## CARACTERISTIQUES DU COMPORTEMENT THERMIQUE ET DYNAMIQUE AU VOISINAGE DES DISCONTINUITES

**Résumé**—Une analyse asymptotique est appliquée pour étudier le comportement fondamental des champs de température et de vitesse au voisinage de l'arête d'un coin. On insiste sur les conditions physiques sous lesquelles le gradient de température devient singulier au sommet du coin. Ces conditions sont sensibles aux conditions thermiques imposées sur les faces du coin. Pour des problèmes de convection naturelle, on trouve que les $r$-dépendances des grandeurs du champ dans la région proche de l'arête sont déterminées par le problème de *valeurs propres* pour le champ de température, tandis que les vitesses d'écoulement sont déterminées par un problème de valeurs *limites*. La situation inverse existe pour les problèmes de convection forcée. Une discussion détaillée est donnée pour l'extension des solutions de proximité de l'arête aux problèmes plus compliqués, en conjonction avec l'utilisation des méthodes d'éléments finis.

## WÄRME- UND IMPULSTRANSPORT IN DER UMGEBUNG VON DISKONTINUITÄTEN

**Zusammenfassung**—In der vorliegenden Arbeit wird mit Hilfe einer asymptotischen Analyse das grundlegende Verhalten von Temperatur- und Geschwindigkeitsfeldern in der Umgebung einer Keilspitze untersucht. Besonderes Augenmerk gilt dabei den physikalischen Bedingungen, unter denen der Temperaturgradient des Strömungsfeldes an der Keilspitze singulär wird. Es zeigt sich, daß diese Bedingungen stark von den thermischen Bedingungen an der Keiloberfläche beeinflußt werden. Weiterhin zeigt sich bei Problemen der natürlichen Konvektion, daß der Verlauf der Feldgrößen in radialer Richtung in der Nähe der Spitze durch das Eigenwert-Problem für das Temperaturfeld bestimmt wird, während die Eigen-Zustände für die Strömungsgeschwindigkeiten durch das Grenzwertproblem bestimmt werden. Für erzwungene Konvektion ergibt sich die umgekehrte Situation. Abschließend wird die Möglichkeit der Ausweitung der Lösungen für die Umgebung der Spitze auf kompliziertere Probleme unter Einbeziehung der Methode der finiten Elemente detailliert diskutiert.

## ТЕПЛОВЫЕ И ДИНАМИЧЕСКИЕ ХАРАКТЕРИСТИКИ ТЕЧЕНИЯ В ОКРЕСТНОСТИ РАЗРЫВА НЕПРЕРЫВНОСТИ

**Аннотация**—С помощью асимптотического анализа исследуются фундаментальные тепловые и динамические характеристики обтекания вершины клина. Особое внимание уделяется динамическим условиям, при которых температурный градиент поля течения у вершины клина становится сингулярным. Найдено, что они зависят от тепловых условий, налагаемых на поверхности клина. Для естественной конвекции получено, что зависимость параметров поля от величины $r$ вблизи вершины клина находится из решения задачи на собственные значения для температурного поля, в то время как собственные состояния для скоростей течения определяются из решения краевой задачи. В случае вынужденной конвекции наблюдается обратная ситуация. Приводится также подробное обсуждение возможности обобщения решений для области вблизи вершины клина на более сложные задачи методом конечных элементов.